

Quark Models of Baryon Masses and Decays

Simon Capstick

*Department of Physics, Florida State University
Tallahassee, FL, USA 32306*

Abstract:

The description of baryon resonance masses and decays in the constituent quark model is outlined, with emphasis on the potential-model approach combined with the 3P_0 pair-creation model of strong decays. This approach allows the estimation of branching fractions for baryon states missing in πN elastic scattering analyses but expected to be present in electromagnetic production. Prospects for the discovery of hybrid baryons are discussed. A subjective list of the most important corrections required to this approach is presented.

1 Introduction

Although many baryon resonances have been seen already in $\pi N \rightarrow \pi N$, $\pi\pi N$, ΛK , *etc.*, many of these states cannot be considered well known. Difficult multi-channel analyses are required to find evidence for resonances from the data, which is necessarily incomplete. Models also predict more states than have been seen in the analyses, and there is a focused effort to discover evidence for as many as possible of these ‘missing’ states in new data from the reactions γN , $e^- N \rightarrow \pi N$, $\pi\pi N$, ηN , ωN , $K\Lambda$, $K\Sigma$, *etc.*

The exploration of known and novel resonances which analysis of this new data will allow has important consequences for our understanding of the nature of low-energy hadronic states. The various QCD-based models disagree on the spectrum and even the relevant degrees of freedom and so the number of excitations. There is controversy about the nature of the short-range interactions between the quarks, and the presence of tensor and spin-orbit interactions. QCD also predicts gluonic excitations which have the same quantum numbers as conventional three-quark states, but which have not so far been seen. All of the states are broad and often overlap. It is a unique challenge to those building models of the fundamental excitations and of the reactions to unravel this physics.

Such a program does not directly test QCD. Currently, *ab-initio* approaches like lattice-QCD are finding good masses for ground-state baryons within the quenched approximation, and full-QCD calculations of these masses are underway [1]. Calculations are also underway of P -wave baryon masses. However, it will remain difficult to predict with lattice QCD the masses and decay branches of the third and fourth $P_{11} N_{\frac{1}{2}}^+$ or $P_{13} N_{\frac{3}{2}}^+$

excited states, for example. The reason for the interest in these highly-excited conventional states is that, as we shall see, establishing their presence rules out models with strong diquark clustering, and the lightest gluonic excitations are likely to have the same quantum numbers.

What this program does test are QCD-based models, which are based on interpreted consequences of QCD. These include potential models, chiral perturbation theory, a collective model based on spectrum-generating algebra, large- N_c expansions, and recently relativistic field-theoretic models based on QCD. This work focuses on the description of baryon masses and decays using potential models.

2 Potential models

In this approach the effective degrees of freedom are constituent quarks, treated symmetrically, unlike those in quark-diquark [2] and collective [3] models. These constituent quarks move in two- and three-body potentials. Initial formulations were non relativistic and based on the Schrödinger equation [4], although many authors now use the relativistic kinetic energy [5] (with a lower constituent quark mass) and some introduce relativistic corrections [6] in the potentials. The dynamical problem is solved by expanding the wave function in a large basis, generally the harmonic-oscillator basis, which has many advantages. It is also possible to use a basis which interpolates between the Coulomb and linear eigenfunctions expected from the short and long-distance behavior of the spin-independent potential, respectively [7]. Once the Hamiltonian matrix has been constructed, it can be diagonalized to find the spectrum and wave functions, and the size of the basis increased until a reasonable convergence of the spectrum is attained.

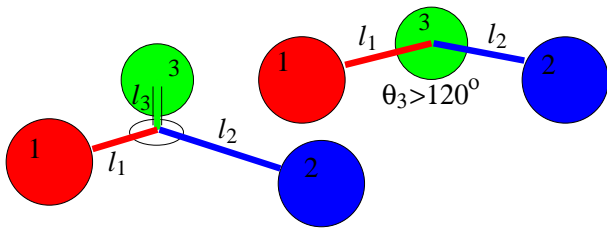


Figure 1: String configurations leading to the confining potential $V_{\text{conf}} = b \sum_i l_i$ in baryons.

Two cases are illustrated in Fig. 1, that where all of angles in the triangle made by joining the quarks are less than 120° , or where one of the angles is larger than 120° . In the first case the sum of the string lengths is minimized when the angles at the junction are all 120° , and in the second it is when the junction is over the quark where the large angle resides. In both cases the confining potential is the sum of the string lengths times the string tension $b \simeq 1.0$ GeV/fm, and it is this potential which is used in modern baryon spectrum calculations.

Quarks are known to exchange gluons with a coupling which is weak at short distances. The short distance potential between the quarks is modeled using this one-gluon exchange interaction as a guide. An alternate model (OPE) uses the exchange of an octet of pseudoscalar mesons [8], with the motivation that the short-distance dynamics of constituent quarks should be governed by dynamical chiral-symmetry breaking. The

A popular model of confinement in baryons uses flux-tubes or strings attached to the quarks and to a junction, combined with the adiabatic approximation, where the strings are assumed to adjust rapidly to the quark motion. A potential is generated by minimizing the string length for each set of quark positions. Two

one-gluon-exchange interaction is similar to the hyperfine interaction between the proton and the electron in the hydrogen atom, with contact and tensor pieces, although it is much stronger. It is responsible for the approximately 300 MeV splitting of the $\Delta(1232)$ and the nucleon. There are also spin-orbit interactions implied by the one-gluon exchange interaction, and spin-orbit interactions due to Thomas-precession in the confining potential are present regardless of the source of the short-distance interactions.

More recent models generally use the relativistic kinetic energy for the quarks and a quark mass of about 220 MeV for the light quarks. The relativized model [6] also applies momentum-dependent relativistic corrections to the confining and short-distance potentials. The wave functions are then expanded in a large (often harmonic-oscillator) basis, and the resulting Hamiltonian matrix is then diagonalized to find the spectrum and wave functions.

As a relevant illustration of this technique, there are three radially-excited harmonic oscillator spatial states, one in each of the two relative coordinates and one unique to the three-body system proportional to the dot product of the two relative coordinates ($\boldsymbol{\rho} \cdot \boldsymbol{\lambda}$). When combined into states of definite exchange symmetry, these make up a symmetric state and a pair of mixed-symmetry states, two of which are illustrated in Fig. 2. When these $L^P = 0^+$ states are combined with the mixed-symmetry quark-spin $S = \frac{1}{2}$ and totally symmetric $S = \frac{3}{2}$ states, the result is five states nominally in the $N = 2$ oscillator band (but note the potential is not harmonic). These are two $N_{\frac{1}{2}}^{1+}$ states, a $\Delta_{\frac{1}{2}}^{1+}$ state, a $N_{\frac{3}{2}}^{3+}$ state, and a $\Delta_{\frac{3}{2}}^{3+}$ state. Some of these states have been seen on pion-nucleon elastic scattering. These are the Roper resonance $N_{\frac{1}{2}}^{1+}(1440)$, its analog $\Delta_{\frac{3}{2}}^{3+}(1600)$, and $N_{\frac{1}{2}}^{1+}(1710)$.

Decay models based on the elementary-meson emission [9] or the 3P_0 pair-creation model [10] can explain why the other states have not been seen—they have small $N\pi$ couplings—and can predict alternate final-state channels in which they are likely to be seen. In one-gluon exchange models the Roper resonance is lighter than the other positive-parity excited states due to a strongly negative contact interaction like that in the proton, and it is also split from the other positive-parity states by the anharmonic nature of the confining potential [4]. When treated properly, without resort to perturbation theory in the large anharmonic perturbation, the Roper resonance becomes much lighter than the other positive parity excited states, but not light enough to explain its position in the spectrum below the lowest (at 1520 MeV) of the negative-parity non-strange excited states. The next P_{11} state, $N_{\frac{1}{2}}^{1+}(1710)$, is in roughly the right position in the spectrum.

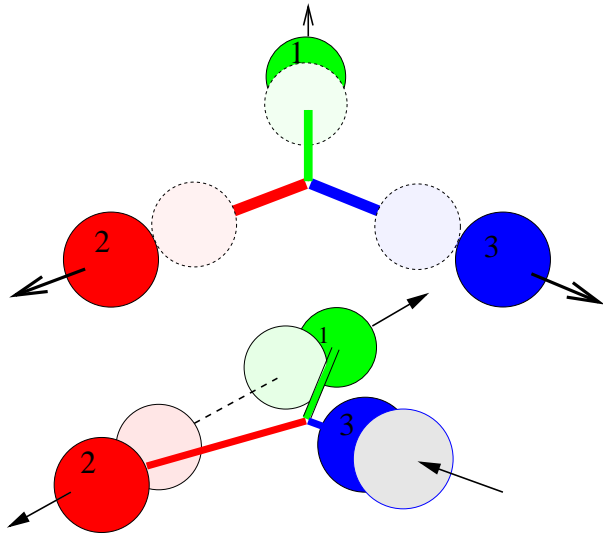


Figure 2: Symmetric radially excited spatial state corresponding to the Roper resonance, and one of the two mixed-symmetry radial states.

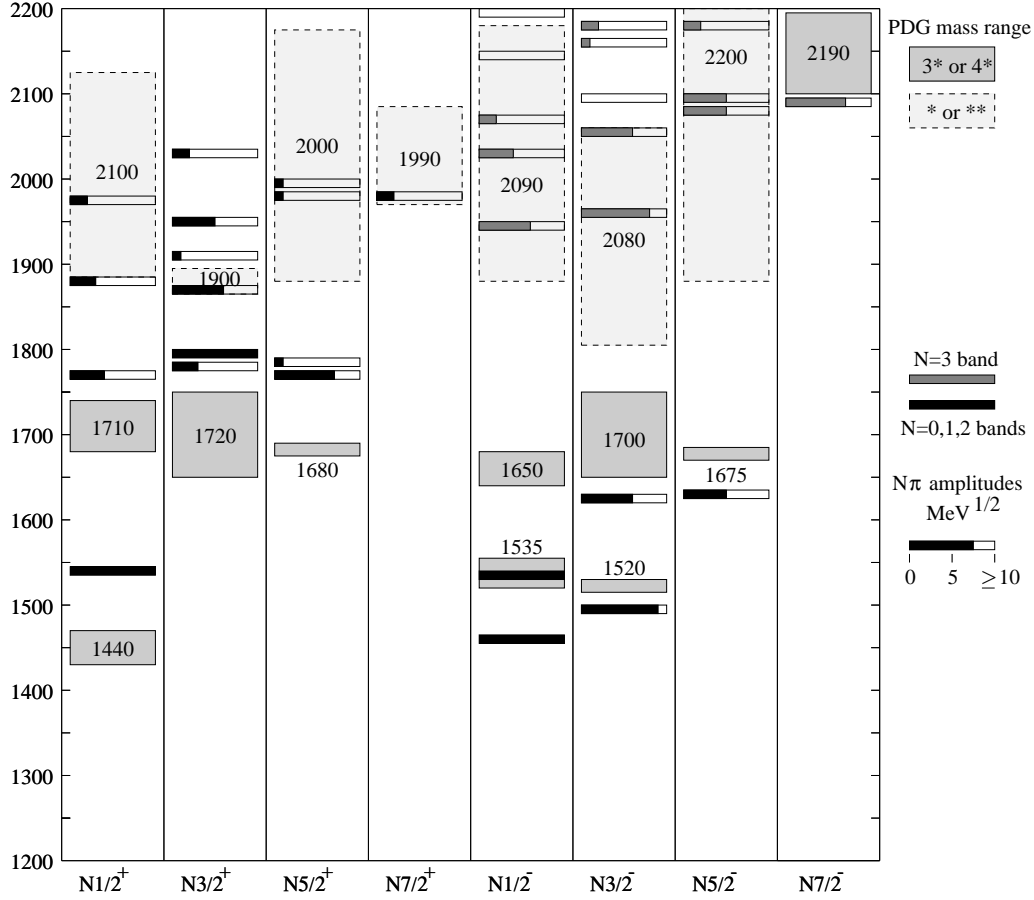


Figure 3: Calculated masses and $N\pi$ decay amplitudes for nucleon resonances below 2200 MeV from Refs. [6, 10], compared to the range of central values for resonances masses from the PDG [11], which are shown as boxes. The boxes are lightly shaded for one and two star states and heavily shaded for three and four star states. Predicted masses are shown as a thin bar, with the length of the shaded region indicating the size of the $N\pi$ amplitude.

Models with OPE-based short-distance interactions explain the low position of this state as due to the flavor-dependence of the resulting contact interaction [8]. However, the Roper resonance is very broad (roughly 350 MeV width), and neither of these approaches takes into account shifts in its mass due to self-energy corrections from baryon-meson loops, which can naively be expected to be of the order of the width. It is therefore not clear whether 100 MeV discrepancies in any spectrum will allow conclusions to be made until this rather difficult problem is consistently dealt with, for all the states in the spectrum.

Masses for nonstrange baryon states below 2200 MeV calculated in this way are shown in Figures 3 and 4, along with $N\pi$ decay amplitudes [10] (their squares give the $N\pi$ partial widths) for each state. The calculated masses are shown as thin bars, and the length of the shaded part of each bar is proportional to the $N\pi$ decay amplitude strength. Also shown in these figures are boxes showing the range in the central value of the mass of resonances quoted by the Particle Data Group [11] (along with their best estimate of the mass), which are compiled from partial-wave analyses of mainly $N\pi$ elastic and inelastic scattering data.

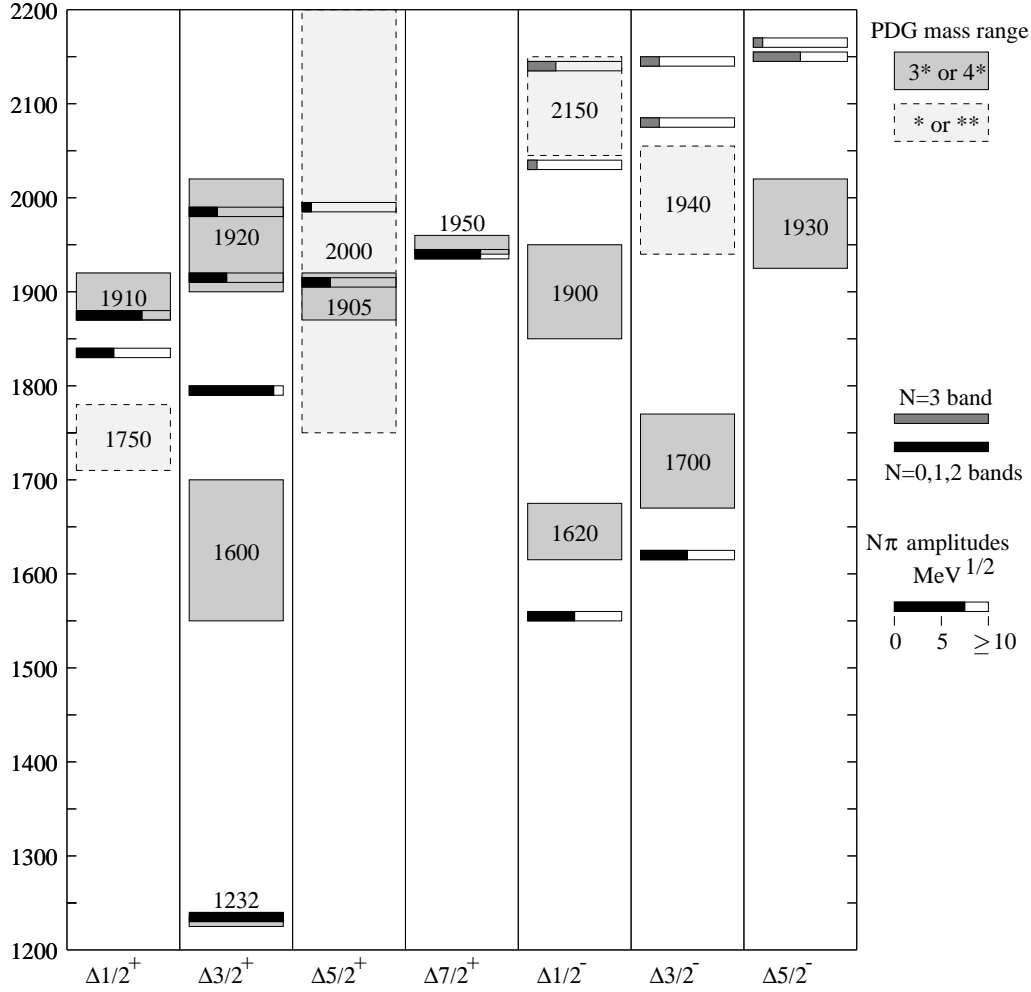


Figure 4: Model masses and $N\pi$ decay amplitudes for Δ resonances below 2200 MeV from Refs. [6, 10], compared to the range of central values for resonances masses from the PDG [11]. Caption as in Fig. 3.

It is clear that low-lying well separated states with substantial $N\pi$ widths are those likely to have been seen in the analyses, and that model states with small $N\pi$ couplings are either poorly established resonances, or not present at all in the analyses. Models which describe the degrees of freedom in baryons at low energy as quarks and diquarks have fewer degrees of freedom and so fewer excitations, so the discovery of additional positive parity excited states (and the confirmation of some existing states) predicted by models which treat the quarks symmetrically could rule out this possibility.

Further insight into the nature of the short-distance interactions between quarks can be found from a consideration of the nature of the spin-orbit and tensor interactions in baryons. Although the cancellation of the two-body parts of the one-gluon exchange (OGE) spin-orbit interactions and those arising from Thomas precession in the confining potential can be arranged [4], spin-orbit splittings are still too large in non relativistic OGE-based models. In the relativized model it is shown that it is possible to have small spin-orbit interactions in baryons due to relativistic effects [6]. This problem is not solved

by the elimination of the spin-orbit forces due to the short-distance interactions, such as in OPE-based models, as this to a large extent is required to cancel against those from the confining potential [12].

Pseudoscalar exchange (OPE) models of the short-distance interactions between quarks have tensor interactions which are very different from those arising from OGE. These interactions have important consequences for the tensor mixings between states such as the $N_{\frac{1}{2}}^{-}(1535)$ and $N_{\frac{1}{2}}^{-}(1650)$, which are strong. The mixings arising from OGE explain why the lower of these two states has a large branch [4] to $N\eta$, which is not the case for mixings found using OPE. Some form of vector exchange, such as gluon exchange or the exchange of two pions in the form of a vector meson [13], is required to describe the details of the strong decays of these states.

Finally, it is clear that OPE-based descriptions of the baryon spectrum cannot reproduce the reasonable unification of baryon and meson physics provided by OGE-based models. They cannot produce hyperfine mixing in mesons where it is needed, and imply unphysical OZI-violating mixings in isoscalar mesons [4]. It is, perhaps, natural [14] to exclude a description of meson states in a model where bound quarks interact by exchanging those same meson states.

Interesting and different physics can be accessed by studying states containing one (Σ and Λ) or more (Ξ) strange quarks. The presence of the strange quark breaks degeneracies present in the nonstrange spectrum and so there are more negative-parity ($L = 1$) excited states. Our knowledge of the spectrum from partial-wave analyses is limited to the ground states Λ , Σ , and $\Sigma^*(1385)$, and about half of the negative-parity excited states and a few of the low-lying positive-parity states predicted by constituent quark models. The spin-orbit partners $\Lambda(1405)_{\frac{1}{2}}^{-}$ and $\Lambda(1520)_{\frac{3}{2}}^{-}$ provide an interesting challenge for quark models, which need to suppress spin-orbit splittings elsewhere in the spectrum to agree with the analyses. These states are predicted to be roughly degenerate in potential models. Because of this poor description in the constituent quark model they been described as $\bar{K}N$ bound states. It is also possible that their large mass splitting arises from corrections to their masses from $qqq(\bar{q}q)$ configurations, as the lightest state lies just below threshold for decay to $\bar{K}N$. Note that OPE models can be adjusted to accommodate this splitting with explicitly flavor-dependent contact interactions (not just through the mass dependence of the hyperfine interaction, as in OGE-based models).

There is information on only a few excited Ξ states extracted from the data, which include the ground states Ξ and Ξ^* , and a few negative-parity excited states. For this reason it is important to search for information on excited Ξ states. There is recent evidence from Jefferson Laboratory of a signal for Ξ states in $e^-p \rightarrow \Xi KK$.

3 Hybrid baryons

The discovery of hybrid baryons is complicated by the fact that the quantum numbers of baryons with excited glue are the same as those of conventional three-quark excitations. Using the flux-tube picture of the confining potential described above, it is possible [15] to describe light hybrid baryons as states where the quarks move in a potential described by an excited state of the glue. This is very different from earlier $qqqg$ models [16] of hybrid baryons, where a gluon and three quarks are confined to a bag.

For fixed positions \mathbf{r}_i of the three quarks, the flux tubes are allowed to move. This is modeled by the motion of the junction, and by transverse motion of the strings relative to their equilibrium directions, as in Fig. 5. By means of an analytic calculation with a bead at the junction and a single bead on each of the three strings, it was shown that a reasonable approximation to the ground-state and first-excited-state energy of the string for each quark position can be found by examining only the junction motion. The strings simply follow the motion of the junction. The adiabatic potentials corresponding to the ground state of the string, $V_B(\mathbf{r}_1, \mathbf{r}_2, \mathbf{r}_3)$, and the the first excited state of the string, $V_H(\mathbf{r}_1, \mathbf{r}_2, \mathbf{r}_3)$, are found by a four-parameter variational calculation, for all quark positions.

The difference of these potentials is then added to the Hamiltonian for the three quark problem, and the energies of the lightest hybrid baryons are then found by solving the three-quark dynamical problem as before, but with the excited string Hamiltonian. It can be shown that the string excitations have orbital angular momentum and parity 1^+ , so that when combined with the lowest energy quark

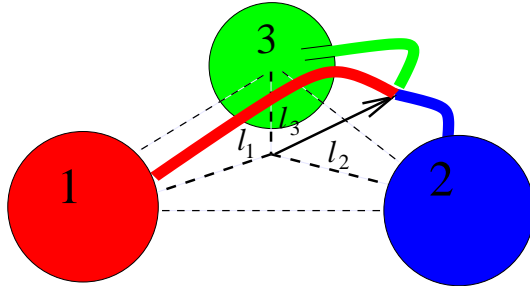


Figure 5: General motion of the flux tubes (strings) in a hybrid baryon.

$L = 0$ and $S = \frac{1}{2}$ or $\frac{3}{2}$, the resulting lowest-lying states are $N_{\frac{1}{2}}^{1^+}$ and $N_{\frac{3}{2}}^{3^+}$ at roughly 1870 MeV, with a model error of about ± 100 MeV. There are also $\Delta_{\frac{1}{2}}^{1^+}$, $\Delta_{\frac{3}{2}}^{3^+}$, and $\Delta_{\frac{5}{2}}^{5^+}$ states at about 2075 MeV with the same estimated error. In the bag model [16] there is a $N_{\frac{5}{2}}^{5^+}$ excited state and no $\Delta_{\frac{5}{2}}^{5^+}$ state, and the lightest states are at about 1500 MeV, significantly lighter than these flux-tube model calculated masses.

Referring back to Figs. 3 and 4, we see that these new states are predicted by this flux-tube model to lie in a region of the spectrum where there are several missing conventional three-quark excitations. Given that these states are likely to mix with the conventional excitations (through corrections to the adiabatic approximation outlined above), it is important that a careful and detailed analysis of these partial waves is carried out with an eye towards establishing more states than are possible without exciting the flux-tubes. It may also be possible to distinguish hybrids based on their electromagnetic excitation amplitudes [17] and strong-decay signatures.

4 Baryon strong decays

It is not enough to find a state in a model with a mass similar to one seen in analyses of scattering experiments (and so listed by the Particle Data Group). In addition, it is necessary to explain why a state should be seen, usually (for nonstrange states) in $N\pi \rightarrow X$, and conversely why states present in the model which have not been seen are missing in the analyses. Popular models of these strong couplings are based on string breaking by the creation of a $q\bar{q}$ pair with vacuum quantum numbers. This model is referred to as the 3P_0 model [18], as a such a quark and antiquark necessarily have relative $L = 1$ and $S = 1$ combined to $J^{PC} = 0^{++}$. Models of meson decays preferentially create

| State | Γ | $N\pi$ | $\Delta\pi$ | $N\rho$ | $N^*\pi$ | $\Delta^*\pi$ | $N\eta$ | $N\omega$ | $\Delta\eta$ | ΛK | ΣK | $\Sigma^* K$ |
|---------------------------------------|----------|--------|-------------|---------|----------|---------------|---------|-----------|--------------|-------------|------------|--------------|
| $[N_{\frac{1}{2}}^{1+}]_4(1880)$ | 150 | .05 | .49 | .03 | .00 | .00 | .18 | .14 | .00 | .00 | .09 | .00 |
| $[N_{\frac{1}{2}}^{1+}]_5(1975)$ | 50 | .08 | .47 | .14 | .01 | .00 | .00 | .22 | .00 | .03 | .01 | .04 |
| $[N_{\frac{3}{2}}^{3+}]_2(1870)$ | 190 | .20 | .12 | .02 | .01 | .02 | .26 | .11 | .00 | .00 | .26 | .00 |
| $[N_{\frac{3}{2}}^{3+}]_3(1910)$ | 390 | .00 | .75 | .03 | .01 | .01 | .00 | .17 | .00 | .00 | .02 | .01 |
| $[N_{\frac{3}{2}}^{3+}]_4(1950)$ | 140 | .12 | .43 | .11 | .00 | .01 | .00 | .28 | .00 | .03 | .01 | .01 |
| $[N_{\frac{3}{2}}^{3+}]_5(2030)$ | 90 | .04 | .57 | .15 | .00 | .01 | .00 | .16 | .00 | .01 | .00 | .06 |
| $[N_{\frac{5}{2}}^{5+}]_2(1980)$ | 270 | .01 | .89 | .02 | .00 | .01 | .00 | .03 | .00 | .00 | .00 | .05 |
| $[N_{\frac{5}{2}}^{5+}]_3(1995)$ | 190 | .00 | .51 | .33 | .00 | .01 | .04 | .08 | .00 | .00 | .00 | .02 |
| $[N_{\frac{7}{2}}^{7+}]_1(2000)$ | 50 | .13 | .53 | .03 | .00 | .02 | .21 | .06 | .00 | .00 | .02 | .00 |
| $[\Delta_{\frac{1}{2}}^{1+}]_1(1835)$ | 310 | .05 | .63 | .20 | .01 | .01 | .00 | .00 | .07 | .00 | .03 | .00 |
| $[\Delta_{\frac{3}{2}}^{3+}]_4(1985)$ | 220 | .05 | .44 | .25 | .00 | .00 | .00 | .00 | .17 | .00 | .05 | .03 |
| $[\Delta_{\frac{5}{2}}^{5+}]_2(1990)$ | 350 | .00 | .56 | .10 | .00 | .00 | .00 | .00 | .28 | .00 | .00 | .05 |

Table 1: Total widths Γ and branching fractions for missing nonstrange baryons, from Refs. [10, 20]. States are labeled by their spin, parity, principal quantum number, and model mass [6]. Here $N^*\pi$ means $N_{\frac{1}{2}}^{1+}(1440)\pi$, $\Delta^*\pi$ means $\Delta_{\frac{3}{2}}^{3+}(1600)\pi$, and Σ^*K means $\Sigma_{\frac{3}{2}}^{3+}(1385)K$. Branching fractions are upper bounds, as discussed in the text.

this pair along the string connecting the quarks.

Progress has been made in understanding this model at the microscopic level [19]. Certain meson decays can result in two relative angular momenta for the final state mesons (S and D -waves, for example), and the ratio of the amplitudes for these decays depends minimally on anything but the structure of the decay vertex. The model of Ackleh, Barnes and Swanson (ABS) creates the quark pair by an interaction with a quark in the decaying meson of the same kind as that which is responsible for that meson's structure. ABS show that this interaction resembles 3P_0 and that the comparison with these ratios favors 3P_0 over the creation of a pair with gluon (3S_1) quantum numbers, for example.

The application of the 3P_0 model to baryon strong decays explains why some of the states predicted by OGE-based models are missing in analyses of the scattering data, which is because they have small couplings to the $N\pi$ channel. Such selection rules may not apply to electromagnetic production of such states, and this model can be used to predict the strongest decay channels for these missing states. This analysis depends not only on the form of the decay operator but also on the model wave functions used for the baryons. A two-parameter model fit to $N\pi$ decays has been used [20] to predict the $\Delta\pi$, $N\rho$, $N\eta$, $N\eta'$, $N\omega$, $N(1440)\pi$, $\Delta(1600)\pi$, $\Delta\eta$, and $\Delta\omega$ decays of excited baryon states. In addition, decays to YK states have been examined, where Y is a hyperon Λ , Σ , $\Sigma^*(1385)$, $\Lambda(1405)$, or $\Lambda(1520)$, and K is a kaon or K^* . These calculations show that it should be possible to discover 'missing' baryon states in several of these channels, especially those with thresholds in the region where these excited positive-parity states lie.

The total widths and branching fractions to nonstrange and strange final states calculated in this way for missing and poorly established nonstrange baryons in the low-lying (nominally $N = 2$) positive-parity bands are shown in Table 1. Branching fractions to $\Delta\omega$, $N\eta'$, $\Lambda_{\frac{1}{2}}^{1-}(1405)K$, and $\Lambda(1520)_{\frac{3}{2}}^{3-}K$ are omitted as they are never larger than 0.01. Note

that these branching fractions should be considered as upper bounds, as there are final states which may have substantial branches, such as $N^*\pi$, where N^* is a negative-parity excited state, which are not included in the total width. Model results for branching fractions are likely to be more reliable than those for the total widths, as they are ratios and some model uncertainties cancel out. Table 1 shows clearly that these states have small $N\pi$ branches and that they may be easy to see in $N\pi\pi$ final states such as $\Delta\pi$ and $N\rho$, as in other channels like $N\eta$ [21] and $N\omega$. Branching fractions into strange final states are predicted to be somewhat smaller, with a few exceptions, but information on these channels can be considered complementary to that of non-strange final states, and so will likely be very useful.

5 Conclusions

One-gluon-exchange based potential models, when combined with the 3P_0 strong decay model, adequately describe diverse features of excited baryon and meson physics. They have been applied to the spectra, strong decays, and electromagnetic couplings of baryons such as photocouplings and electroproduction amplitudes (not mentioned here). The results of these calculations show reasonable agreement with resonance properties extracted from analyses of data.

These models are not covariant, although they include relativistic corrections, and electroproduction amplitudes have been calculated with light-cone based relativistic models. We need new relativistic structure models based on QCD. More importantly, constituent quark models generally ignore Fock-space components of baryons beyond simple qqq configurations. This is equivalent to the quenched approximation in lattice QCD, or to assuming that baryon-meson intermediate states have no effects on the physics of the baryon resonances. This is obviously an important missing ingredient, given that none of these states are narrow. In addition, these models need to take into account excitations of the glue.

The parallel development of a detailed and comprehensive data analysis program is required to extract meaningful results for new and poorly established baryons from exciting new data coming from several sources. These results will certainly challenge our understanding of the physics of excited baryons, and may lead to a new level of understanding of the low-energy features of QCD.

References

- [1] C. R. Allton *et al.* [UKQCD Collaboration], Phys. Rev. **D60**, (1999) 034507; S. Aoki *et al.* [CP-PACS Collaboration], Phys. Rev. Lett. **84**, (2000) 238.
- [2] G. R. Goldstein, TUFTS-TH-G88-5 *Presented at Workshop on Diquarks, Turin, Italy, Oct 24-26, 1988.*
- [3] R. Bijker, F. Iachello and A. Leviatan, Annals Phys. **236**, (1994) 69; Phys. Rev. **C54**, (1996) 1935; Annals Phys. **284** (2000) 89.
- [4] N. Isgur and G. Karl, Phys. Rev. **D18**, (1978) 4187; *ibid.* **D19**, (1979) 2653.

- [5] L.Y. Glozman, W. Plessas, L. Theussl, R.F. Wagenbrunn and K. Varga, PiN Newslett. **14**, (1998) 99.
- [6] S. Capstick and N. Isgur, Phys. Rev. **D34**, (1986) 2809.
- [7] J. Carlson, J. Kogut and V. R. Pandharipande, Phys. Rev. **D27**, (1983) 233; R. Sartor and F. Stancu, Phys. Rev. **D31**, 128 (1985); *ibid.* **D33**, (1986) 727.
- [8] L.Y. Glozman and D.O. Riska, Phys. Rept. **268**, (1996) 263.
- [9] R. Koniuk and N. Isgur, Phys. Rev. **D21**, (1980) 1868.
- [10] S. Capstick and W. Roberts, Phys. Rev. **D47**, (1993) 1994.
- [11] D. E. Groom *et al.*, Eur. Phys. J. **C15** (2000) 1.
- [12] N. Isgur, nucl-th/9908028.
- [13] R. F. Wagenbrunn, L. Y. Glozman, W. Plessas and K. Varga, Nucl. Phys. **A666-667**, (2000) 29c.
- [14] L. Y. Glozman, Nucl. Phys. **A663-664**, (2000) 103.
- [15] S. Capstick and P. R. Page, Phys. Rev. **D60**, (1999) 111501.
- [16] T. Barnes and F. E. Close, Phys. Lett. **B123**, (1983) 89; E. Golowich, E. Haqq and G. Karl, Phys. Rev. **D28**, (1983) 160; C. E. Carlson, T. H. Hansson and C. Peterson, Phys. Rev. **D27**, (1983) 1556.
- [17] Z. Li, V. Burkert and Z. Li, Phys. Rev. **D46**, (1992) 70.
- [18] A. Le Yaouanc, L. Oliver, O. Pene and J. C. Raynal, Phys. Rev. **D18**, (1978) 1591.
- [19] E. S. Ackleh, T. Barnes and E. S. Swanson, Phys. Rev. **D54** (1996) 6811.
- [20] S. Capstick and W. Roberts, Phys. Rev. **D49** (1994) 4570; *ibid.* **D57** (1998) 4301; *ibid.* **D58** (1998) 074011.
- [21] S. Capstick, T. S. Lee, W. Roberts and A. Svarc, Phys. Rev. **C59** (1999) 3002